

Neutrino signatures of the supernova - gamma ray burst relationship

Soebur Razzaque,¹ Peter Mészáros¹ and Eli Waxman²

¹*Dpt Astronomy & Astrophysics, Dpt Physics, Pennsylvania State Univ., University Park, PA 16802, USA*

²*Department of Condensed Matter Physics, Weizmann Institute of Science, Rehovot 76100, Israel*

(Dated: February 2, 2008)

We calculate the TeV-PeV neutrino fluxes of gamma-ray bursts associated with supernovae, based on the observed association between GRB 030329 and supernova SN 2003dh. The neutrino spectral flux distributions can test for possible delays between the supernova and the gamma-ray burst events down to much shorter timescales than what can be resolved with photons. As an illustrative example, we calculate the probability of neutrino induced muon and electron cascade events in a km scale under-ice detector at the South Pole, from the GRB 030329. Our calculations demonstrate that km scale neutrino telescopes are expected to detect signals that will allow to constrain supernova-GRB models.

PACS numbers: 95.85.Ry, 96.40.Tv, 98.70.Rz, 98.70.Sa

I. INTRODUCTION

Gamma-ray bursts (GRB) have recently been shown to be associated with supernova (SN) events. This is based, most notably, on the burst GRB 030329, in whose optical afterglow the supernova (labelled SN 2003dh) photometric and spectral signatures show up 9.6 days [1] after the γ -ray trigger. This late brightening of the supernova is caused by the large initial opacity to optical photons of the envelope of the exploding supernova. The collapse of the stellar core is thought to lead, for progenitor stellar masses in excess of $30 M_\odot$, to a blackhole responsible for the GRB (e.g. [2] for a review), while for less massive progenitors it leads to a rotating neutron star, typically detectable as a pulsar. A question of great interest is whether the supernova explosion of a progenitor in excess of $\sim 30 M_\odot$ can lead to a black hole promptly (on a timescale comparable to the core collapse free-fall time), or else after some delay, during which an initial pulsar accretes additional gas which falls back onto it from the envelope [3]. In the extreme version of this scenario the collapse to a black hole is delayed by weeks to months [4]. Optical observations cannot test the time off-set which characterizes this scenario to an accuracy better than a few days [1, 5, 6], due to observational difficulties and uncertainties in modeling the diffusive photon transport in the dynamically evolving envelope. Neutrinos, however, are not subject to the very long diffusion times of photons, due to their much lower opacities, and should provide a much tighter time-tracking of the collapse. While thermal (MeV) neutrinos produced in the collapse are presently undetectable except from the very nearest galaxies, ultra-high energy (\gtrsim TeV) neutrinos from GRBs are expected to be detectable from cosmological distances with kilometer scale Cherenkov detectors [7, 8, 9, 10] or giant air-shower detector [11]. Here we calculate the \gtrsim TeV neutrino signatures associated with the collapse of massive stellar progenitors of GRB, both in the case where a supernova envelope is ejected simultaneously with, or sometime before, the GRB event. We calculate the resulting muon and electron cascade events

in kilometer scale sub-ice detectors, and discuss the characteristic signatures associated with various time off-sets between the GRB and the SN.

II. OBSERVATIONS AND MODEL

The GRB 030329 is located at the coordinates $\alpha = 10^h 44^m 50.03^s$, $\delta = +21^\circ 31' 18.1''$ (J2000) [1]. The distance of the burst at redshift $z \approx 0.17$ is $D \approx 10^{27.3} D_{27.3}$ cm for an $\Omega_m = 0.3$, $\Omega_\Lambda = 0.7$ and $H_0 = 75$ km s^{-1} Mpc $^{-1}$ cosmology. The observed GRB duration is $\Delta t \sim 30 \Delta t_{30}$ s with 10^{-4} erg/cm 2 fluence in the 30-400 keV range. The peak flux is 7×10^{-6} erg cm $^{-2}$ s $^{-1}$ with 1.2 s duration. The isotropic γ -ray luminosity $L_\gamma^{\text{iso}} \sim 10^{51} L_{\gamma,51}$ erg/s is then approximately the same as the typical value for long bursts.

We take the progenitor star to have an original mass of $\sim 30 - 40 M_\odot$, which subsequently lost its H envelope leaving behind a He core of $\sim 14 M_\odot$ in its presupernova phase. The He core has initially a smaller radius of $\sim 1.2 R_\odot$, for a solar metallicity star, but grows larger later in its He burning stage. The density profile of the star can be roughly estimated as $\rho = \rho_*(R_*/r - 1)^n$, where $\rho_* = 2$ g/cm 3 and $R_* \sim 10^{11}$ cm in the presupernova phase [12]. In case of $n \approx 3$, for radiative envelope, $\rho \approx 10^{-3}$ g/cm 3 for $r \sim 0.9 R_*$.

The supernova SN 2003dh is similar to SN 1998bw, with a similar explosion energy estimated as $E_{sn} = (2 - 5) \times 10^{52}$ erg, and an ejected supernova remnant (SNR) shell velocity of $\approx 0.1c$ [5]. We consider here two scenarios: first, the SN takes place 0.1-8 days prior to the (electromagnetically detected) GRB event; and second, both the SN and the GRB occur simultaneously. The neutrino fluxes from these two scenarios differ significantly, as discussed in the following section.

III. NEUTRINO FLUX COMPONENTS

High energy neutrinos are created from photomeson ($p\gamma$) and proton-proton (pp) interactions by the shock accelerated protons in the GRB shocks. In the γ -ray prompt phase of the GRB, neutrinos are produced through $p\gamma$ interactions [13]. A precursor component arises, due to pp and $p\gamma$ interactions, when the GRB jet is burrowing its way through the star [14, 15]. If an SNR shell is ejected days before the GRB event, an extra component is added to the prompt phase neutrino flux because of pp and $p\gamma$ interactions in the shell [16, 17]. Afterglow reverse shocks also generate high energy neutrinos through $p\gamma$ interactions [18, 19]. We consider each of these flux components, in the framework of astrophysical models described in Sec. II, below.

A. Burst

The Thomson depth of the GRB internal shocks at a radius r_{sh} is $\tau_{\text{Th}} \approx \sigma_{\text{Th}} L_{\gamma}^{\text{iso}} \delta t / (4\pi r_{\text{sh}}^2 \Gamma m_p c^2)$, where $\delta t \sim 10^{-3} \delta t_{-3}$ s is the variability time and $\Gamma \approx 300 \Gamma_{300}$ is the bulk Lorentz factor. Solving for $r_{\text{sh}} = r_{\text{thin}}$ at $\tau_{\text{Th}} = 1$, we get the shock radius at which the GRB jet becomes optically thin as

$$r_{\text{thin}} \approx 10^{12} \left(\frac{L_{\gamma,51} \delta t_{-3}}{\Gamma_{300}} \right)^{1/2} \text{ cm}. \quad (1)$$

The optical depth for $p\gamma \rightarrow \Delta$ at threshold with observed $\epsilon_{\gamma}^{\text{burst}} \approx 0.5$ MeV peak synchrotron photons is

$$\tau_{p\gamma} \sim 10 \left(\frac{\sigma_{p\gamma}}{\sigma_{\text{Th}}} \right) \left(\frac{\epsilon_{\gamma}^{\text{burst}}}{0.5 \text{ MeV}} \right)^{-1} \Gamma_{300}. \quad (2)$$

Correspondingly, the proton to pion conversion efficiency in the internal shocks is $f_{\pi}^{\text{burst}} \approx 1 f_{\pi,0}^{\text{burst}}$. The neutrino break energy for $p\gamma$ interactions with peak synchrotron photons is

$$E_{\nu,b}^{\text{burst}} \approx 2 \times 10^6 \left(\frac{\epsilon_{\gamma}^{\text{burst}}}{0.5 \text{ MeV}} \right)^{-1} \Gamma_{300}^2 \text{ GeV}; \quad (3)$$

assuming 5% of the proton energy goes to a neutrino in each interaction at the Δ -resonance ($E_p \epsilon_{\gamma}^{\text{burst}} = 0.2 \text{ GeV}^2$ in the comoving frame). Neutrinos below this energy interact with synchrotron photons above $\epsilon_{\gamma}^{\text{burst}} \approx 0.5 \text{ MeV}$ which follow a typical power law distribution $dN_{\gamma}/dE_{\gamma} \propto E_{\gamma}^{-2}$. At ultra-high energies, neutrino production is suppressed due to synchrotron losses of secondary pions and muons produced from $p\gamma$ interactions. The maximum pion synchrotron break energy, from equipartition magnetic field with equipartition fraction $\xi_B = 0.01 \xi_{B,-2}$, is

$$E_{\pi, sb}^{\text{burst}} \approx 3.8 \times 10^8 \left(\frac{L_{\gamma,51} \Gamma_{300} \delta t_{-3}}{\xi_{B,-2}} \right)^{1/2} \text{ GeV}. \quad (4)$$

Assuming the luminosity of internal shock-accelerated protons in the GRB is $L_p \sim \kappa L_{\gamma,51}$, the power-law distribution of protons is

$$\frac{d^2 N_p}{dE_p dt} \approx 6.2 \times 10^{53} \frac{\xi_p \kappa L_{\gamma,51}}{E_p^2} \text{ GeV}^{-1} \text{ s}^{-1}. \quad (5)$$

Here $\xi_p \lesssim 1$ is the fraction of protons accelerated and $\kappa \gtrsim 1$. The corresponding neutrino spectrum at earth [$\Phi_{\nu} = d^2 N_{\nu}/dE_{\nu} dt = (4\pi D^2)^{-1} d^2 N_p/dE_p dt$] is

$$E_{\nu}^2 \Phi_{\nu} = 3.1 \times 10^{-3} \frac{f_{\pi,0}^{\text{burst}} \xi_p \kappa L_{\gamma,51}}{D_{27.3}^2} \times \begin{cases} (E_{\nu}/E_{\nu,b}^{\text{burst}}); & E_{\nu} < E_{\nu,b}^{\text{burst}} \\ 1; & E_{\nu,b}^{\text{burst}} > E_{\nu} > E_{\nu, sb}^{\text{burst}} \\ (E_{\nu}/E_{\nu, sb}^{\text{burst}})^{-1}; & E_{\nu} > E_{\nu, sb}^{\text{burst}} \end{cases} \times \text{GeV cm}^{-2} \text{ s}^{-1}, \quad (6)$$

where $E_{\nu, sb}^{\text{burst}} \approx 9.4 \times 10^7 \text{ GeV}$ is the maximum synchrotron energy for neutrinos from Eq. (4).

B. Afterglow

The GRB afterglow arises as the jet fireball ejecta runs into the ambient medium [the inter-stellar medium (ISM) or a pre-ejected stellar wind], driving a blast wave ahead into it and a reverse shock back into the GRB jet ejecta. This (external) reverse shock takes place well beyond the internal shocks, at a radius $r_e \sim 4\Gamma_e^2 c \Delta t \sim 10^{17.3} \Gamma_{250}^2 \Delta t_{30} \text{ cm}$ [18]. Here $\Gamma_e \approx 250 \Gamma_{250}$ is the bulk Lorentz factor of the ejecta after the partial energy loss incurred in the internal shocks. Neutrinos are produced in the external reverse shock due to $p\gamma$ interactions of internal shock accelerated protons predominantly with synchrotron soft x-ray photons produced by the reverse shock. The characteristic photon energy in the observer frame for the ISM case is [18]

$$\epsilon_{\gamma}^{\text{glow}} \approx \frac{0.3}{\xi_{B,-2}^{3/2} n_0 L_{\gamma,51}^{1/2} \Delta t_{30}} \text{ keV}, \quad (7)$$

where $0.01 \xi_{B,-2}$ is the magnetic field equipartition fraction from typical afterglow fits and $1 n_0 \text{ cm}^{-3}$ is the inter-stellar medium density. The corresponding neutrino break energy, for $p\gamma$ interactions, is

$$E_{\nu,b}^{\text{glow}} \approx 2 \times 10^9 \left(\frac{\epsilon_{\gamma}^{\text{glow}}}{0.3 \text{ keV}} \right)^{-1} \Gamma_{250}^2 \text{ GeV}. \quad (8)$$

The efficiency of pion conversion from $p\gamma$ interactions in GRB afterglows is $f_{\pi}^{\text{glow}} \approx 0.1 f_{\pi,-1}^{\text{glow}}$; smaller than in internal shocks [18]. The afterglow neutrino spectrum [Afterglow (ISM) case] is then

$$E_{\nu}^2 \Phi_{\nu} = 3.1 \times 10^{-3} \frac{f_{\pi,-1}^{\text{glow}} \xi_p \kappa L_{\gamma,51}}{D_{27.3}^2}$$

$$\begin{aligned} & \times \begin{cases} (E_\nu/E_{\nu,b}^{\text{glow}}); & E_\nu < E_{\nu,b}^{\text{glow}} \\ (E_\nu/E_{\nu,b}^{\text{glow}})^{1/2}; & E_\nu > E_{\nu,b}^{\text{glow}} \end{cases} \\ & \times \text{GeV cm}^{-2} \text{ s}^{-1}. \end{aligned} \quad (9)$$

Note that ultra-high energy neutrinos from afterglows are not suppressed due to pion synchrotron losses, because of the smaller magnetic fields at the larger radius of the external shock (in contrast to internal shocks).

The estimate in Eq. (9) is derived under the assumption that the jet expands into a medium with a density typical to that of the interstellar medium, $n \simeq 1 \text{ cm}^{-3}$. However, in the case of a massive star progenitor the jet may be expanding into a wind, emitted by the progenitor prior to its collapse. In this case, the density of the surrounding medium, at the external shock radius, may be much higher than that typical to the interstellar medium. For a wind with mass loss rate of $10^{-5} M_\odot \text{ yr}^{-1}$ and velocity of $v_w = 10^3 \text{ km/s}$, the wind density at the typical external shock radius would be $\simeq 10^4 \text{ cm}^{-3}$. The higher density implies a lower Lorentz factor of the expanding plasma during the reverse shocks stage, and hence a larger fraction of proton energy lost to pion production. Protons of energy $E_p \gtrsim 10^{18} \text{ eV}$ lose all their energy to pion production [18, 19], and the resulting neutrino flux [Afterglow (wind) case] is approximately given by [20]

$$\begin{aligned} E_\nu^2 \Phi_\nu & \approx 3.1 \times 10^{-3} \frac{\xi_p \kappa L_{\gamma,51}}{D_{27.3}^2} \min \left(1, \frac{E_\nu}{10^{17} \text{ eV}} \right) \\ & \times \text{GeV cm}^{-2} \text{ s}^{-1}. \end{aligned} \quad (10)$$

The neutrino flux is expected to be strongly suppressed at energies $E_\nu > 10^{19} \text{ eV}$, since protons are not expected to be accelerated to energies $E_p \gg 10^{20} \text{ eV}$.

C. Supranova

If the SN explosion resulting in a SNR shell ejection takes place hours to few days prior to the GRB (“supranova” scenario), then one expects an extra neutrino component, due to GRB-accelerated proton interactions taking place in the pre-ejected SNR shell, which is in addition to the burst and afterglow components. Optical observations suggest a maximum of 2-8 days delay [5, 6], and are compatible with no delay.

Assuming the SN energy $E_{\text{sn}} \approx 2 \times 10^{52} E_{52.3} \text{ erg}$ converts to kinetic energy with the observed velocity $v_{\text{snr}} \approx 3 \times 10^9 v_{9.5} \text{ cm/s}$ of the SNR shell, the mass of the shell is $M_{\text{snr}} \approx 2 - 3 M_\odot$. For our calculation, we take $M_{\text{snr}} = 2.2 m_{2.2} M_\odot$. The typical distance reached by the SNR shell is $R_{\text{snr}} \approx 10^{14.4} v_{9.5} t_d \text{ cm}$ in t_d days. We assume an isotropic distribution of shell matter with $\delta = \Delta R_{\text{snr}} / R_{\text{snr}} = 0.1 \delta_{-1}$ width for $t_d \gtrsim 1 \text{ day}$. For younger SNR shells, the matter may be taken to be approximately isotropically distributed between the progenitor star and up to R_{snr} .

One of the two dominant photon components trapped inside the SNR shell consists of photons from the SN shock with black body temperature of [16]

$$\epsilon_\gamma^{\text{sn}} \approx 5 \frac{E_{52.3}^{1/4} \delta_{-1}^{1/3} R_*^{1/4}}{v_{9.5} t_d} \text{ eV}. \quad (11)$$

Another photon component may arise, for $t_d \gtrsim 1 \text{ day}$, because of a magnetohydrodynamic (MHD) wind which impacts the inner shell radius driving a forward shock through the shell. With an MHD wind luminosity of $L_{\text{mhd}} \sim 10^{46} L_{\text{m46}} \text{ erg/s}$ from a fast-rotating pulsar resulting from the SN, the thermalized photon energy in the SNR shell is

$$\epsilon_\gamma^{\text{m}} \approx 17 \frac{L_{\text{m46}}^{1/4} \delta_{-1}^{1/4}}{v_{9.5}^{3/4} t_d^{1/2}} \text{ eV}. \quad (12)$$

The optical depths for $p\gamma$ interactions of these two photon components are

$$\begin{aligned} \tau_{p\gamma}^{\text{sn}} & \approx 8 \times 10^4 \frac{E_{52.3}^{3/4} \delta_{-1}^{1/3}}{R_*^{1/4} v_{9.5} t_d} \\ \tau_{p\gamma}^{\text{m}} & \approx 10^4 \frac{L_{\text{m46}}^{3/4} \delta_{-1}^{1/4}}{v_{9.5}^{1/2} t_d^{1/2}}. \end{aligned} \quad (13)$$

High energy protons escaping from GRB internal shocks (with an escape factor $\eta_p < 1$) may interact with thermalized SN and MHD photons in the SNR shell. The corresponding neutrino threshold energies are

$$\begin{aligned} E_{\nu,th}^{\text{sn}} & \approx 5.7 \times 10^8 \frac{v_{9.5} t_d \Gamma_{300}}{E_{52.3}^{1/4} \delta_{-1}^{1/3} R_*^{1/4}} \text{ GeV}. \\ E_{\nu,th}^{\text{m}} & \approx 1.7 \times 10^8 \frac{v_{9.5}^{3/4} t_d^{1/2} \Gamma_{300}}{L_{\text{m46}}^{1/4} \delta_{-1}^{1/4}} \text{ GeV}. \end{aligned} \quad (14)$$

in the observer frame. Protons below Δ production threshold energies may undergo pp interactions in the SNR shell. The mean optical depth for such pp interactions is $\langle \tau_{pp} \rangle \approx 60 \zeta_{sh} m_{2.2} / (v_{9.5} t_d)^2$ for an average 60 mb total pp cross section. Here $\zeta_{sh} \lesssim 1$ is the fraction of cold protons inside the SNR shell. The maximum neutrino energy from pion synchrotron energy losses in the SNR shell magnetic field is

$$E_{\nu,sh}^{\text{snr}} \approx 7.6 \times 10^9 \left(\frac{\delta_{-1} v_{9.5} t_d^3}{\xi_B m_{2.2}} \right)^{1/2} \Gamma_{300} \text{ GeV}. \quad (15)$$

We calculate the neutrino flux from pp interactions, below the proton threshold energy at Δ production, for times $t_d \gtrsim 1 \text{ day}$ as

$$\begin{aligned} E_\nu^2 \Phi_\nu & = 1.2 \times 10^{-2} \frac{\eta_p \zeta_{sh} f_{pp,0} \kappa L_{\gamma,51} E_\nu^2}{D_{27.2}^2} \\ & \times \int_{E_p^{\text{mx}}} dE_p \frac{M_\nu(E_p)}{E_p^2} \text{ GeV cm}^{-2} \text{ s}^{-1}; \\ M_\nu(E_p) & = \frac{7}{2} \Theta \left(\frac{1}{4} \frac{m_\pi}{\text{GeV}} \gamma_{\text{cm}} \leq \frac{E_\nu}{\text{GeV}} \leq \frac{1}{4} \frac{E_p}{\text{GeV}} \right); \end{aligned} \quad (16)$$

where $f_{pp,0} \approx 1$ is the neutrino conversion efficiency in pp interactions and $E_p^{mx} \approx 20 \times E_{\nu,th}^{sn,m}$ from Eq. (14). The $p\gamma$ neutrino flux component is similar to the burst neutrino flux and we calculate it as

$$E_\nu^2 \Phi_\nu = 3.1 \times 10^{-3} \frac{f_{\pi,0}^{snr} \eta_p \kappa L_{\gamma,51}}{D_{27.3}^2} \times \begin{cases} 1; & E_{\nu, sb}^{snr} > E_\nu > E_{\nu, th}^{sn,m} \\ (E_\nu / E_{\nu, sb}^{snr})^{-1}; & E_\nu > E_{\nu, sb}^{snr} \end{cases} \times \text{GeV cm}^{-2} \text{ s}^{-1}; \quad (17)$$

where $f_{\pi,0}^{snr} \approx 1$ is the fraction of proton energy lost to pions. We assume that all protons ($\eta_p = 1$) below and 10% protons ($\eta_p = 0.1$) above the proton threshold energy $20 \times E_{\nu, b}^{\text{burst}}$ [Eq. (3)] escape the GRB internal shocks in Eqs. (16) and (17) to calculate neutrino flux.

For $t_d \ll 1$ day the calculation needs to include pion energy losses, due to inverse Compton scatterings in a high density photon field, before they decay to neutrinos.

D. Precursor

A precursor neutrino component (~ 30 s duration) is generated while the GRB jet is still burrowing its way out of the stellar envelope. We have calculated this component for a similar progenitor model in detail elsewhere [15]. There we considered a presupernova star which had either lost ($R_* \sim 10^{11}$ cm) or retained its H envelope ($R_* \sim 10^{12}$ cm). For the simultaneous SN-GRB scenario, these presupernova models are the same. In the “supranova” scenario, the status of the progenitor is uncertain, since numerical simulations which might provide guidance are not available so far. One possibility is that, except for the ejected envelope, the rest of the star becomes the pulsar plus possibly a disk prior to collapse to a black hole leading to the GRB, so that a precursor may not be seen before the GRB event, since there is no stellar core to burrow through. A second possibility (depending on the delay) is that, at the time of the GRB, there is some fraction of the stellar gas which is not part of the ejected shell at radii intermediate between the shell and the central object, which could lead to a precursor resembling the above progenitor cases. The gas column density traversed by the jet is likely to be smaller than in the simultaneous SN case, reducing the pp contribution and producing a weaker precursor.

We have plotted muon neutrino flux components at earth from GRB 030329 associated with SN 2003dh in Fig. 1. The “Precursor” components arrive ~ 30 s prior to the “Burst” component, and are expected in the case when the GRB and the SN events take place simultaneously. The “Precursor I” signal assumes the presupernova stellar radius is $\approx 10^{11}$ cm. The “Precursor II” signal is calculated assuming the star has an envelope, or the He/C/O core has expanded, out to a radius $\sim 10^{12}$ cm before the onset of the GRB event. The “Afterglow

(ISM)” and “Afterglow (wind)” components are calculated when the GRB jet materials run into lower density ISM and a higher density wind respectively. While the burst and the afterglow components are based on generic GRB features, the “Supranova” components are highly model dependent. We have plotted the supranova components assuming that 10% of the shock accelerated protons escape internal shocks to interact with the SNR shell which is up to 8 day old, according to current observational limits. We have plotted the “Supranova” components for 0.1 d (short dashed curve), 1 d (long dashed curve) and 8 d (dotted curve). Note a reduced $p\gamma$ flux contribution ($E_\nu \gtrsim 10^7$ GeV) for the 0.1 d case due to inverse Compton losses of pions. The duration of all components are $\Delta t \approx 30 \Delta t_{30}$ s.

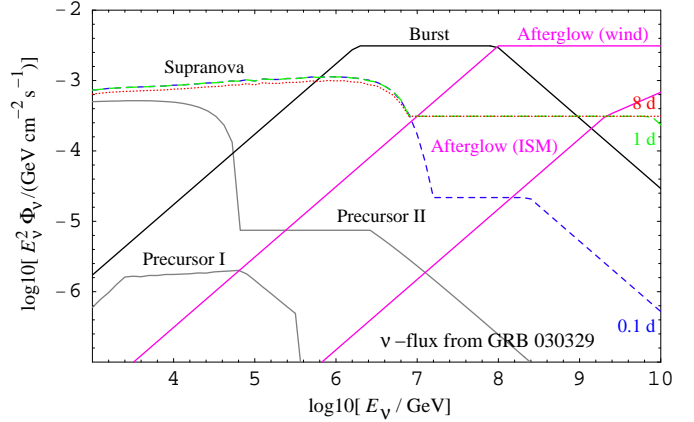


FIG. 1: Muon neutrino flux components from GRB 030329 and the associated SN 2003dh. Possible “Supranova” components are plotted for 0.1 d (short dashed curve), 1 d (long dashed curve) and 8 d (dotted curve) delays of the SN event prior to the GRB. The “Precursor” signals are calculated in the case when the GRB and the SN events take place simultaneously. The “Precursor I” signal is for a progenitor star which has lost its H envelope. The “Precursor II” signal assumes that the star has retained an H envelope, or the He/C/O core has expanded, out to a radius $\sim 10^{12}$ cm before the onset of GRB event. The internal shock “Burst” component [13] is shown by full dark lines. The “Afterglow (ISM)” and “Afterglow (wind)” components, also shown as full dark lines, are calculated for expansion into a lower density surrounding ISM, and a higher density wind, respectively.

IV. DETECTION AT EARTH

Neutrino detection at earth requires a large volume of material because of a small neutrino-nucleon (νN) cross section [21, 22, 23, 24]. Ice Cherenkov detectors such as AMANDA [25], IceCube [7], RICE [8] and ANITA [9]; water Cherenkov detector such as ANTARES [10]; and extended air shower detector such as AUGER [11] are poised to detect cosmic neutrinos in different energy ranges. Several authors have recently calculated

expected neutrino events, based on generic flux models, from individual GRBs [26]. Here we calculate the number of neutrino events that one can expect from GRB 030329 and the associated SN 2003dh, based on flux models described in Sec. III, in an under-ice Cherenkov detector located at the South Pole as an example.

Neutrinos from a point source in the northern hemisphere travel through a substantial amount of earth material to reach a detector at the South Pole. Given a certain zenith angle θ , the column depth of material is $Z(\theta) = \int_0^L \rho(r; \theta, l) dl$, where $\rho(r; \theta, l)$ is the density of earth's interior, based on the Preliminary Reference Earth Model [27], at a depth l and the corresponding earth's interior radius r . The upper limit of integration is the chord length $L = 2R_\oplus \cos \theta$ where $R_\oplus \approx 6371$ km is earth's outer radius. The interaction length for neutrinos inside earth is $\Lambda_{\nu N}(E_\nu) = N_A \sigma_{\nu N}^{\text{eff}}(E_\nu)$, where N_A is the Avogadro's number and the effective cross section is given by

$$\sigma_{\nu N}^{\text{eff}}(E_\nu) = \sigma_{\nu N}^{\text{CC}}(E_\nu) + \sigma_{\nu N}^{\text{NC}}(E_\nu) - \int_{E_\nu}^\infty dE'_\nu \frac{\Phi'_\nu}{\Phi_\nu} \frac{d\sigma_{\nu N}^{\text{NC}}}{dE'_\nu}(E'_\nu, E_\nu); \quad (18)$$

for an incident neutrino flux Φ_ν . Here $\sigma_{\nu N}^{\text{CC}}$ and $\sigma_{\nu N}^{\text{NC}}$ are the total charge current (CC) and neutral current (NC) cross sections respectively and the third term corresponds to the neutrino regeneration phenomenon due to NC interactions which degrade a neutrino to lower energies [22, 28]. For simplicity we have ignored neutrino regeneration in Eq. (18), and the effective cross section is then the sum of CC and NC cross section $\sigma_{\nu N}^{\text{eff}} \approx \sigma_{\nu N}^{\text{CC}} + \sigma_{\nu N}^{\text{NC}} = \sigma_{\nu N}^{\text{tot}}$. The survival probability of a neutrino, from a point source, penetrating through the earth is

$$S(E_\nu) = \exp[-Z(\theta)/\Lambda_{\nu N}(E_\nu)] \approx \exp\left[-N_A \sigma_{\nu N}^{\text{tot}}(E_\nu) \int_0^L \rho(r; \theta, l) dl\right]. \quad (19)$$

We use the total νN cross sections (CC and NC) given in Ref. [24] to calculate the survival probability.

Neutrinos surviving after penetrating earth must interact with nucleons inside the effective detection volume to be detected as an event. Secondary e or μ produced by the CC interaction ($\nu_{e,\mu} + N \rightarrow e, \mu + X$) then lead to either a high energy e -cascade or μ -track from which a Cherenkov signal can be picked up in the radio [29] or optical band [25]. The probability for a $\nu_{e,\mu}$ to interact and produce a secondary e, μ of energy $E_{e,\mu}$ above a minimum value $E_{e,\mu}^{\text{min}}$ in the vicinity of the detector is then

$$P_{e,\mu}(E_\nu) = \frac{1}{\sigma_{\nu N}^{\text{CC}}} \int_{E_{e,\mu}^{\text{min}}}^{E_\nu} dE_{e,\mu} \frac{d\sigma_{\nu N}^{\text{CC}}}{dE_{e,\mu}}(E_\nu, E_{e,\mu}) \times (1 - \exp[-N_A \sigma_{\nu N}^{\text{CC}}(E_\nu) R_{e,\mu}]). \quad (20)$$

Here R_e is the electron range and is essentially the linear dimension of the detector. The muon range is given by the analytic formula

$$R_\mu(E_\mu, E_\mu^{\text{min}}) = \frac{1}{b} \ln \frac{a + bE_\mu}{a + bE_\mu^{\text{min}}} \quad (21)$$

where $a = 2 \times 10^{-3} \text{ GeV cm}^2 \text{ g}^{-1}$ and $b = 4 \times 10^{-6} \text{ cm}^2 \text{ g}^{-1}$ [30]. We have plotted neutrino interaction probabilities, in a km deep under-ice detector, after surviving through earth [$S(E_\nu)P_{e,\mu}(E_\nu)$] from GRB 030329 ($\theta = 68.4^\circ$) in Fig. 2. Because of their longer range, the probability for muon tracks (solid curves) are higher than for electron induced cascades (dashed curves). We have also plotted the probabilities for horizontal and upward neutrino events for comparison.

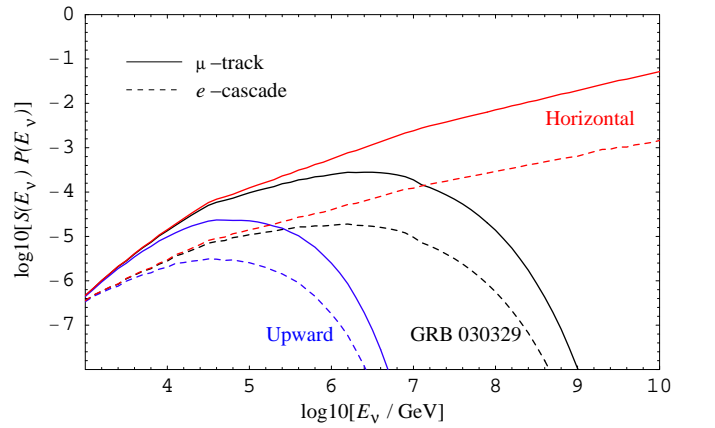


FIG. 2: Probability [$S(E_\nu)P_{e,\mu}(E_\nu)$] of neutrino interaction in the detector volume, after penetrating through earth from GRB 030329, in a km deep under-ice detector at the South Pole. Also shown are the probabilities for upward and horizontal neutrinos for comparison. Probabilities for a muon event and an electron induced cascade event are shown by solid and dashed curves respectively.

The number of neutrino events, given a flux $\Phi_\nu = d^2 N_\nu / dE_\nu dt$, in a detector of effective area A_{eff} is then

$$N_{e,\mu} = A_{\text{eff}} \Delta t \int dE_\nu \frac{d^2 N_\nu}{dE_\nu dt} S(E_\nu) P_{e,\mu}(E_\nu), \quad (22)$$

from Eqs. (19) and (20). We have used a duration $\Delta t = 30 \Delta t_{30}$ s for all fluxes. We have tabulated (see Table I) the expected number of muon tracks and electron cascades from GRB 030329 in an under-ice detector of $A_{\text{eff}} = \text{km}^2$ for different neutrino flux components. We used $E_{e,\mu}^{\text{min}} = 100 \text{ GeV}$ for these calculations.

V. SUMMARY AND DISCUSSION

We have calculated the $\gtrsim \text{TeV}$ neutrino signals from gamma-ray bursts resulting from the collapse of massive stars associated with supernovae, both in the case where

TABLE I: Neutrino events in a km scale under-ice detector at the South Pole from the GRB 030329 and the associated SN 2003dh. We have also calculated events assuming similar GRB-SN with declinations 90° (upward events denoted by \uparrow) and 0° (horizontal events denoted by \rightarrow) cases. We have not considered detector response for our calculation.

Flux Component	TeV-PeV		PeV-EeV	
	μ -track	e -cascade	μ track	e -cascade
Precursor I	$9 \cdot 10^{-3}$	$2 \cdot 10^{-3}$	-	-
	$6 \cdot 10^{-3} \uparrow$	$2 \cdot 10^{-3} \uparrow$	-	-
	$0.01 \rightarrow$	$2 \cdot 10^{-3} \rightarrow$	-	-
Precursor II	4.1	1.1	$3 \cdot 10^{-3}$	$2 \cdot 10^{-4}$
	$2.9 \uparrow$	$0.9 \uparrow$	-	-
	$4.4 \rightarrow$	$1.2 \rightarrow$	$0.01 \rightarrow$	$8 \cdot 10^{-4} \rightarrow$
Burst	1.8	0.2	1.4	0.1
	$0.3 \uparrow$	$0.04 \uparrow$	-	-
	$2.9 \rightarrow$	$0.3 \rightarrow$	$7.6 \rightarrow$	$0.4 \rightarrow$
Afterglow (ISM)	$2 \cdot 10^{-4}$	$2 \cdot 10^{-5}$	$2 \cdot 10^{-4}$	$1 \cdot 10^{-5}$
	$3 \cdot 10^{-5} \uparrow$	$4 \cdot 10^{-6} \uparrow$	-	-
	$2 \cdot 10^{-4} \rightarrow$	$2 \cdot 10^{-5} \rightarrow$	$0.01 \rightarrow$	$5 \cdot 10^{-4} \rightarrow$
Afterglow (wind)	0.03	$3 \cdot 10^{-3}$	0.05	$3 \cdot 10^{-3}$
	$5 \cdot 10^{-3} \uparrow$	$7 \cdot 10^{-4} \uparrow$	-	-
	$0.05 \rightarrow$	$5 \cdot 10^{-3} \rightarrow$	$1.4 \rightarrow$	$0.06 \rightarrow$
Supranova 0.1 d	12.4	2.4	0.5	0.03
	$6.1 \uparrow$	$1.6 \uparrow$	-	-
	$14.9 \rightarrow$	$2.7 \rightarrow$	$1.6 \rightarrow$	$0.1 \rightarrow$
Supranova 1 d	12.4	2.4	0.5	0.03
	$6.1 \uparrow$	$1.6 \uparrow$	-	-
	$14.9 \rightarrow$	$2.7 \rightarrow$	$1.9 \rightarrow$	$0.1 \rightarrow$
Supranova 8 d	10.9	2.2	0.4	0.03
	$5.4 \uparrow$	$1.4 \uparrow$	-	-
	$13.2 \rightarrow$	$2.4 \rightarrow$	$1.7 \rightarrow$	$0.1 \rightarrow$

the supernova occurs simultaneously with, or hours to days in advance of, the γ -ray event. Longer SN-GRB time off-sets of weeks to months as considered in the “supranova” scenario [4], which would have had interesting consequences for the interpretation of GRB afterglows, are ruled out by observations of GRB 030329-SN

2003dh [1, 5, 6]. Shorter off-sets of days to hours, however, which cannot be ruled out by optical observations, could be the signature of a delayed black hole formation from fall-back of gas onto an initial neutron star. Such two-step black hole formation could be expected in intermediate mass ($30M_\odot \lesssim M_* \lesssim 40M_\odot$) stellar progenitor core collapse [3], after delays of fractions of hours to \lesssim day. Within this range, the time off-set is so far poorly constrained due to the approximate nature of the numerical simulations. Thus, any experimental constraints would be very useful, and neutrino signals such as discussed here would be essentially the only way to obtain information about the dynamics of the core collapse. Figure 1 gives the predicted supranova muon neutrino fluxes for a burst such as GRB 030329 assuming three different time delays between the SN and the GRB. For a simultaneous GRB-SN event, these supranova fluxes would be absent.

The detection of \gtrsim TeV neutrino signals from transient sources such as GRBs is basically background free [7]. The number of μ -tracks and e -cascades from the GRB internal shock [Burst and Precursor II components] and from interaction of shock-accelerated GRB protons with the supernova shell (if the later precedes the GRB by hours to days) are certainly above atmospheric background of ~ 0.3 events in the TeV-PeV range. In the PeV-EeV range, ν_μ events from the Burst component should be detectable over zero atmospheric background events. We note, furthermore, that the number of ν_μ events would be doubled in case there is no flavor oscillation. The detection of, or upper limits on, such events could provide important insights both on the collapse dynamics and on the GRB central engine.

Acknowledgements – We thank Alexander Heger for helpful discussion on presupernova star models. This research is supported in part by NSF AST0098416 and NASA NAG5-13286. EW is partially supported by a Minerva grant.

-
- [1] K.Z. Stanek *et al.*, *Astrophys. J.* **591**, L17 (2003).
 - [2] P. Mészáros, *Annu. Rev. Astron. Astrophys.* **40**, 137 (2002).
 - [3] A. MacFadyen, S. Woosley and A. Heger, *Astrophys. J.* **550**, 372 (2001).
 - [4] M. Vietri and L. Stella, *Astrophys. J.* **507**, L45 (1998).
 - [5] T. Matheson *et al.*, *astro-ph/0307435*.
 - [6] J. Hjorth *et al.*, *Nature*, **423**, 847 (2003); K.S. Kawabata *et al.*, *astro-ph/0306155*; R. Willingale *et al.*, *astro-ph/0307561*
 - [7] IceCube Collaboration, J. Ahrens *et al.* *astro-ph/0305196*.
 - [8] RICE Collaboration, I. Kravchenko *et al.*, *Astropart. Phys.* **19**, 15 (2003); I. Kravchenko *et al.*, *astro-ph/0306408*.
 - [9] P. Gorham, in *Ultra high Energy Particles from Space*, Aspen (2002).
 - [10] ANTARES Collaboration, *astro-ph/9907432*.
 - [11] H. Blumer [Pierre Auger Collaboration], *Prog. Part. Nucl. Phys.* **48**, 63 (2002).
 - [12] E. Waxman and P. Mészáros, *Astrophys. J.* **584**, 390 (2003).
 - [13] E. Waxman and J.N. Bahcall, *Phys. Rev. Lett.* **78**, 2292 (1997); E. Waxman and J.N. Bahcall, *Phys. Rev. D* **59**, 023002 (1999).
 - [14] P. Mészáros and E. Waxman, *Phys. Rev. Lett.* **87**, 171102 (2001).
 - [15] S. Razzaque, P. Mészáros and E. Waxman, *Phys. Rev. D* (in press), *astro-ph/0303505*.
 - [16] S. Razzaque, P. Mészáros and E. Waxman, *Phys. Rev. Lett.* **90**, 241103 (2003).
 - [17] D. Guetta and J. Granot, *Phys. Rev. Lett.* **90**, 201103

- (2003); J. Granot and D. Guetta, Phys. Rev. Lett. **90**, 191102 (2003).
- [18] E. Waxman and J.N. Bahcall, Astrophys. J. **541**, 707 (2000).
- [19] Z.G. Dai and T. Lu, Astrophys. J. **551**, 249 (2001).
- [20] E. Waxman, Nucl. Phys. B (Proc. Suppl.) **118**, 353 (2003).
- [21] G. Frichter, D.W. McKay and J.P. Ralston, Phys. Rev. Lett. **74** (1995); G. Frichter, D.W. McKay and J.P. Ralston, Phys. Rev. Lett. **77**, 4107, (1996).
- [22] G.M. Frichter, J.P. Ralston and D.W. McKay, Phys. Rev. D **53**, 1684 (1996).
- [23] R. Gandhi *et al.*, Astropart. Phys. **5**, 81 (1996).
- [24] R. Gandhi *et al.*, Phys. Rev. D **58**, 093009 (1998).
- [25] E. Andres *et al.*, Astropart. Phys. **13**, 1 (2000).
- [26] D. Guetta *et al.*, astro-ph/0302524.
- [27] A. Dziewonsky, Phys. Earth Planet. Interiors **25**, 297 (1981).
- [28] V.S. Berezinskii *et al.*, Sov. J. Nucl. Phys. **43**, 406 (1986).
- [29] E. Zas, F. Halzen and T. Stanev, Phys. Rev. D **45**, 362 (1992). S. Razzaque *et al.*, Phys. Rev. D **65**, 103002 (2002); S. Razzaque *et al.*, astro-ph/0306291; J. Alvarez-Muñiz *et al.*, astro-ph/0206043.
- [30] S.I. Dutta *et al.*, Phys. Rev. D **63**, 094020 (2001);